Advances in Science and Technology Research Journal

Advances in Science and Technology Research Journal 2024, 18(5), 101–112
https://doi.org/10.12913/22998624/190133
ISSN 2299-8624, License CC-BY 4.0

Received: 2024.06.05
Accepted: 2024.07.01
Published: 2024.08.01

A Numerical Study of the Influence of Cone Angle of the Breakout Anchor Head on the Crack Trajectory of the Medium

Andrzej Wójcik[1], Józef Jonak[1], Robert Karpiński[1*], Kamil Jonak[2], Dariusz Prostański[3], Roman Kaczyński[4]

[1] Department of Machine Design and Mechatronics, Faculty of Mechanical Engineering, Lublin University of Technology, ul. Nadbystrzycka 36, 20-618 Lublin, Poland

[2] Department of Technical Informatics, Lublin University of Technology, ul. Nadbystrzycka 38D, 20-618 Lublin, Poland

[3] KOMAG Institute of Mining Technology, ul. Pszczyńska 37, 44-100 Gliwice, Poland

[4] Faculty of Mechanical Engineering, Bialystok University of Technology, ul. Wiejska 45C, 15-351 Białystok, Poland

* Corresponding author's e-mail: r.karpinski@pollub.pl

ABSTRACT

Anchors of various designs are crucial, especially in mining and underground construction, where they stabilise the excavation and prevent the movement of rocks. They make it possible to control the direction of cracking during explosions, limit the dispersion of rock material and minimise damage from vibrations. The use of anchors increases the safety and efficiency of work in difficult geological conditions. The authors propose the use of modified anchor construction for the detachment of rock lumps. The paper presents the results of a numerical analysis carried out using the finite element method (FEM) on the effect of the angle of the anchor conical head of a new breakout design on the formation of the detachment crack trajectory influencing the range and, consequently, the volume of detached rock output. The analysis was carried out with a view to explaining the mechanism of separation of lumps of rock by the anchor treated as a mining tool.

Keywords: undercut/breakout anchor, mining extracting tool; FEM analysis; breakout rock mass, rock cone failure.

INTRODUCTION

Anchors of various designs are mainly used in civil engineering and mining, e.g. for stabilizing slopes, escarpments and underground structures such as tunnels. They are also used to strengthen foundations and to secure deep excavations, for example during the construction of slurry walls. They are crucial in areas where the risk of landslides or other ground displacement is high, providing additional stability and safety [1–3].

Rock excavation with extracting anchors is a safe method that can be used in difficult conditions, such as excavation in a critical installation zone where traditional techniques are risky [4–6]. These anchors are embedded in the rock and then expanded, causing cracks without generating sparks or much heat. Although it may be less effective than explosive methods, extracting anchors provide controlled and safe rock mining [6–8].

The use of numerical methods such as FEM, BEM and neural networks can significantly reduce the amount of physical testing [9–12] and field studies in rock excavation with extracting anchors by enabling advanced simulations and numerical models, optimizing anchor design, reducing risk and uncertainty, and integrating with real-time monitoring systems [13–16]. FEM and BEM allow accurate analysis of rock behavior and neural networks allow to predict results based on previous data [17]. This makes processes faster, cheaper and more efficient, minimizing the need for costly field studies [18–21]. The authors of this study attempt to apply a modified undercutting

anchor design [22], for the detachment of rock elements under unusual conditions of engineering activity, e.g. removing parts of critical structures or carrying out rescue operations in underground mining, in the case of rock fall and lack of space to apply typical solutions in this area. Details of previous experience both in the field and in numerical analyses are presented in [23].

Under typical conditions, the anchors used to date are used for installation in reinforced concrete structures, a variety of technical infrastructure [24–28]. A suitably abundant knowledge has emerged in this area, particularly with regard to the determination of the anchor load capacity (or pull-out force) [29–32], both in individual operation [33] and in the anchor unit [26,34]. For a critical review of the state of knowledge in this area, see [35–37]. Most analyses are carried out using FEM [38–41] or BEM (Boundary Element Method) [42]. The use of the XFEM (eXtended Finite Element Method) algorithm is becoming widespread due to the advantages it offers [43–45]. XFEM is an effective numerical method for solving discontinuous crack propagation problems [46–48], as it overcomes the problem of high-density gridding in areas where stresses and deformations are concentrated and does not require re-gridding during crack propagation. The result of the analysis depends little on the size of the finite elements. Because of this advantage, XFEM is widely recognised as the preferred method for analyzing discontinuous problems [49–51]. For the accuracy of the results obtained from numerical analyses, it is important to estimate the cracking resistance of the rock medium. For such media, however, there is often the problem of determining the crack strength [52–54], hence attempts are made to predict cracking resistance or crack energy using machine learning [55, 56].

The use of HDP-A-type undercutting anchors for rock detachment requires the use of a tool with high pulling force, size and weight [23]. This limits the use of detachment technology by pulling out the anchor, as a sufficiently large space is required for the action. In order to remove these limitations, we have proposed to upgrade the anchor design (Fig.1), allowing the rock breaking process to be carried out in the vicinity of the bottom of the borehole where the anchor is installed, instead of the tear-off process previously used [57].

Figure 1 illustrates the anchor after installation in a borehole made in the rock. As a result of the application of a torque M to the anchor, the value of the relative distance of the anchor elements DY increases, through which the value of the reaction forces in contact between the head elements and the rock increases, leading to the initiation and development of slots and the formation of the so-called cone of damage of the medium. Ultimately, the increasing relative displacement of the anchor elements leads to the detachment of a cone-shaped lump of rock [23, 58, 59].

Due to the change in the damage mechanism of the rock medium, the aim of the presented research was to verify the effect of the head cone angle β (Figure 1), on the propagation of the damage zone including, in particular, the trajectory and potential range of the slot on the free rock surface (which has a significant impact on the volume of the rock lumps to be detached in the proposed breakout technology).

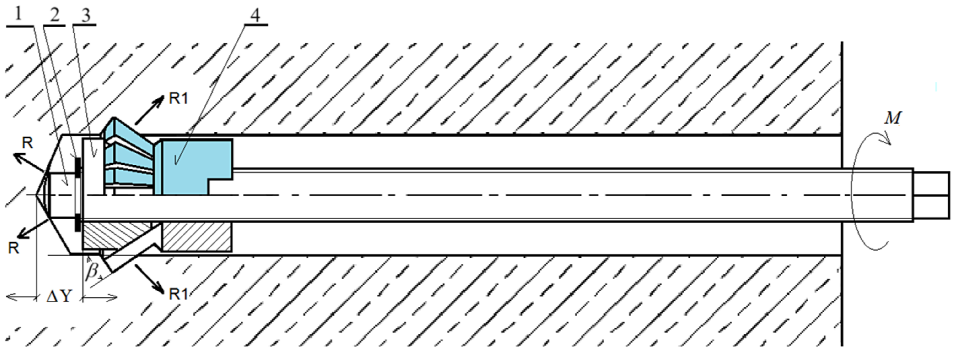

Figure 1. Undercutting and breakout anchor: 1 – the end of the driving bolt resting against the bottom of the rock borehole, 2 – retaining ring, 3, 4 – conical anchor head components (3 – cone nut, 4 – expansion ring), M – the driving torque applied to the driving bolt of the anchor, ΔY – Increase in relative displacement, end of bolt and conical anchor head, R – reaction forces in the contact between the bolt end and the rock at the bottom of the borehole, R_1 – reaction forces in contact between the conical head element and the rock, β – conical head angle

MATERIALS AND METHODS

As described above, in the new breakout anchor designs under consideration, there is a breaking of the rock medium realized by the successive expansion of the anchor head and driving bolt against the rock medium at their points of contact. This differs from the previously studied structures of breakout undercutting anchors. Hence, the subject of the study was the process of destruction of the rock structure under the action of the breakout anchor head. The aim of the study was to determine the effect of changing the load transfer mechanism from the anchor to the rock medium, on the crack trajectory. This has a significant effect on the volume of potentially fractured rock lumps, which is of interest in turn for evaluating the effectiveness of the proposed extraction method. One of the main factors affecting the crack trajectory is the value of the conical head angle β. Hence, the specific objective was to investigate the effect of this angle on crack propagation during the fall of the rock medium, under conditions of load transfer from the anchor to the rock medium that are different from those studied so far. The analysis was carried out numerically using the ABAQUS program (Abaqus 2023, Dassault Systemes Simulia Corporation, Velizy Villacoublay, France) and using the XFEM algorithm (eXtended Finite Method).

The rock medium with the following mechanical parameters was used for the analysis

Type of material

Sandstone: elastic, isotropic. Elastic modulus E =14.276 MPa, Poisson's ratio ν = 0.247, Tensile Strength – f_t = 7.74 MPa.

Anchor material: steel – material: Elastic, Isotropic, Elastic modulus E = 210,000 MPa, Poisson's ratio ν = 0.3.

The coefficient of friction of the steel head against the rock was adopted: μ = 0.2 (studies [60] show that good matching results are obtained for μ = 0.35÷0.4. In numerical studies [61, 62] a good match was obtained for μ = 0.2).

Anchor geometry and process implementation parameters

Anchor mounting depth h_{ef} = 100 mm. Head angle β = 15°, 20°, 25°, 30° (four theoretical cases were analyzed). Hypothetical angle of the cone of damage α = 22,5°.

For the analysis of the cracking process of the rock medium under the impact of the breakout anchor, the typical procedures for determining the conditions for damage initiation and development implemented in the FEM ABAQUS programme were used, i.e:

- damage initiation in rock material: maximal principal stress,
- damage evolution: type: energy, softening linear,
- damage for traction - separation laws: maximal principal stress damage,
- fracture energy E_{Ic} = 0.17 N/mm,
- damage stabilization – cohesive.

A mechanical model of the interaction of the elements of the tested anchor with the rock medium is shown in Figure 2a. A linear connector finite element available in ABAQUS was used to implement the change in relative position of the anchor head and the end of the bolt resting against the bottom of the borehole.

In the zone of interaction of the anchor elements with the rock, the 'surface-to-surface contact' procedure was applied, contact with friction 'Panalty contact', available in ABAQUS. The geometrical parameters of the anchor were assumed to correspond to the dimensions of the HILTI HDP-A-M20 anchor head, hence a geometrical model of the rock medium including the anchor installation hole was constructed for the numerical analysis, as in Figure 3 (due to symmetry, the issue was treated as axisymmetric and analyzed in the axial section of the anchor). The value of the head angle β (15°, 20°, 25°, 30°) was varied, assuming a constant anchor mounting depth (h_{ef} =100 mm), a constant value for the radius of the base of the conical part of the head (= 25.2 mm, as in Fig. 3a) and a constant value for the radius of the hole under the cylindrical part of the anchor (= 18.5 mm, as in Fig. 3a). The dimensions of the rock medium model were taken as width R = 500 mm and height H=300mm, as shown in Figure 3b.

In the critical areas of the rock medium model, a variable node distance was applied at the periphery of the rock medium, as in Fig. 4, condensing it, e.g. in the potential crack initiation zone, i.e. in the zone of interaction between the end of the bolt and the corner of the cone head (Fig. 4a).

The restraints/boundary conditions are shown in Figure 4b. The nodes in the vertical axis of

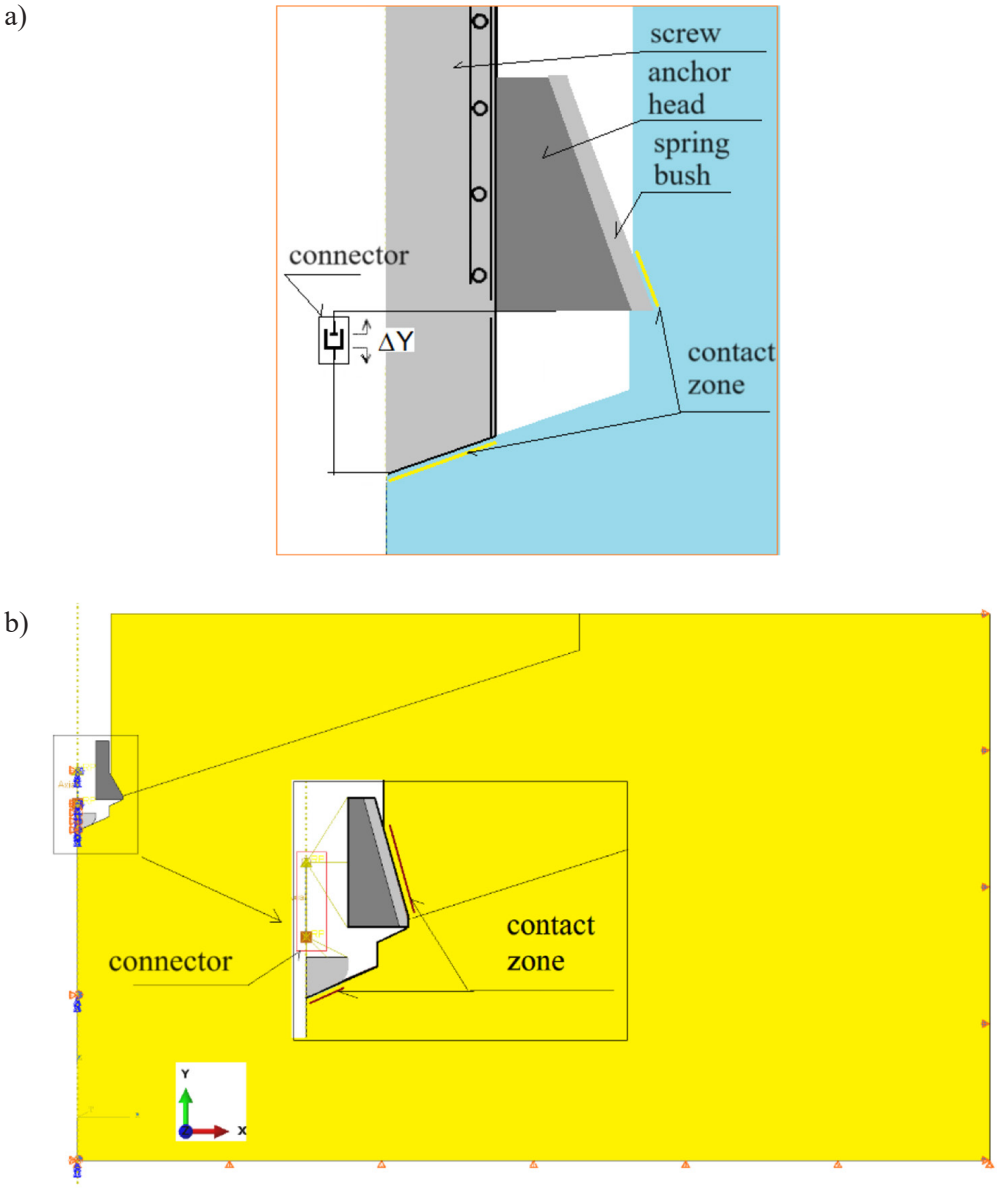

Figure 2. Mechanical model of an undercutting and breakout anchor during rock bursting – (a) model of the connection between the reference nodes of the conical head and the propeller using the connector type finite element available in ABAQUS (b)

the model under the anchor were deprived of all degrees of freedom (U1 = U2 = U3). Restraints nodes in the base of the model – U2 = 0, nodes on the right edge – U1 = 0. There is symmetry about the Y-axis in the model of the rock and reference points associated with the anchor and bolt, hence U1 = U3 = UR2 = 0 (Fig. 4b).

As a result of the automatic grid generator of the ABAQUS software, the final shape of the element grid was obtained, as in Figure 5. As can be seen from the sensitivity analysis carried out previously [57, 63, 64], a grid of this type was the best for the numerical analyses carried out in the subject undertaken.

RESULTS

The results of the analyses carried out are presented in Figures 6–7. Figure 6 illustrates the distribution of the maximum main stresses σ_{max} against the finite element grid and the gap created in the last propagation step, when convergence of the algorithm was still achieved. In the next simulation step, the calculations were coming to a stop (lack of convergence). As can be seen, the trajectory of slots and its extent depend on the value of the anchor head angle β.

In Figure 7, the course of the recorded slots is shown against the finite element grid itself to

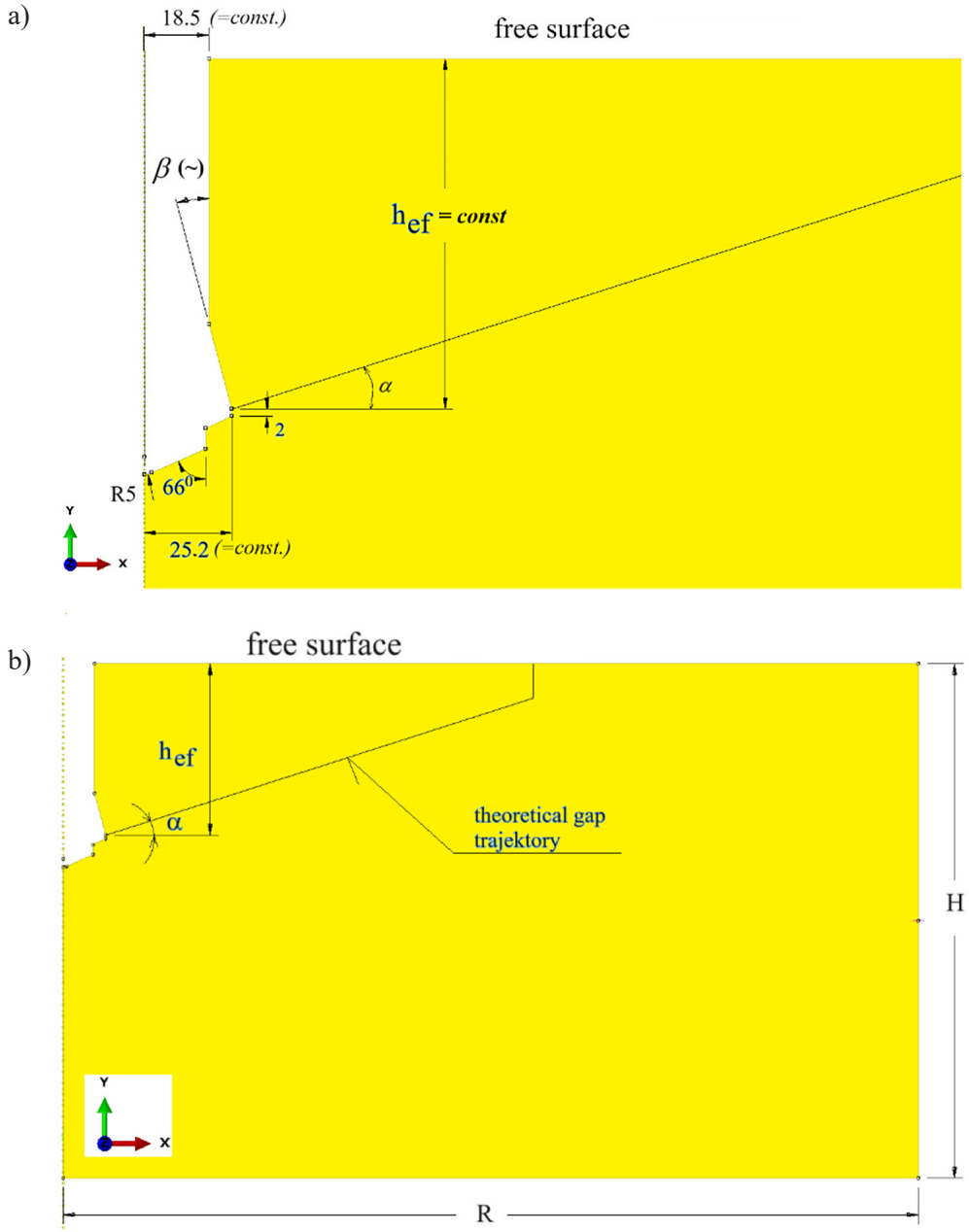

Figure 3. Geometry of the rock medium model including hole and undercut for the anchor, where *a* – hypothetical angle of damage cone

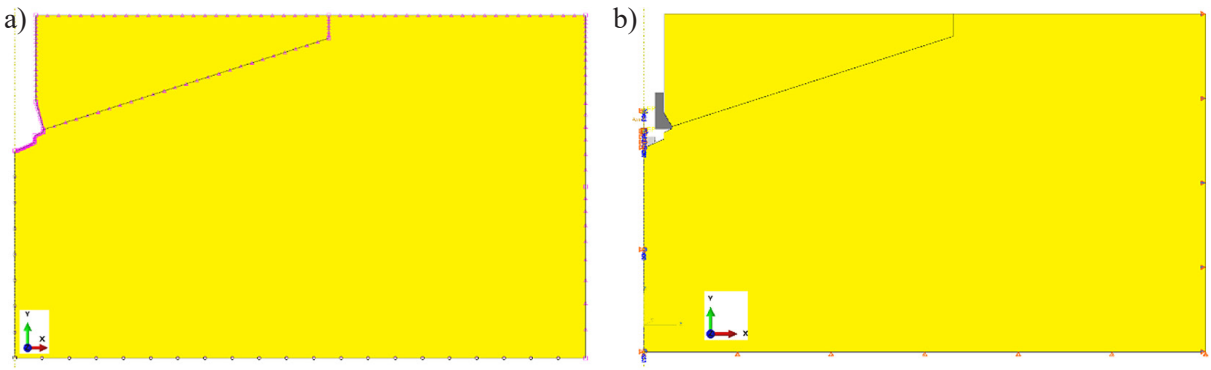

Figure 4. Arrangement of the initial nodes of the finite element grid model on the periphery of the rock model (a), and restraints of the model boundary nodes – (b)

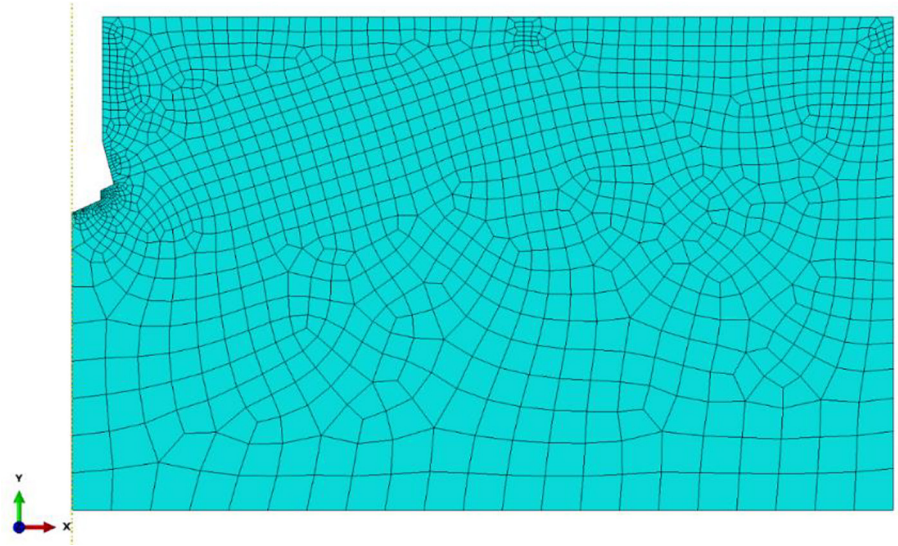

Figure 5. Finite element grid of the rock medium model

enhance the legibility of the drawings. A deformation scale of 2 has been used, which makes the slot more visible by enlarging its opening.

For better illustration and the possibility of more complete comparisons, all the slot courses are summarized in Figure 8. As assumed earlier, the value of the anchor mounting depth h_{ef} and the value of the conical head base radius $\boldsymbol{a}$, were constant. The head angle β was varied in the range 15–30° (only the extreme angle values are marked in the figure).

The simulation results confirmed the occurrence of slot initiation point under the driving bolt end (point A, Fig. 8), as was observed in preliminary studies [57], i.e. differently from the detached undercutting anchors, i.e. at the base of the undercutting head – point B, in Fig. 8 [7, 65]. There are indications that there may be a potential influence of the geometric parameters of the medium model, such as the value of the clearance between the surface of the hole where the anchor is located and the surface of the bolt in the area above the head as well as in the vicinity of the hole bottom and the end of the driving bolt. This aspect may influence the magnitude of deformation from bending of the detached lump (damage cone), the location of the slot initiation and its trajectory. These aspects should be clarified in further studies.

In addition, a general relationship is apparent from Figure 8 that smaller head angles β favour a larger range of slots (measured along the free rock surface). This partly confirms the trends previously observed for the breakout-undercutting anchors illustrated in Figure 9 [7, 65]. In this case, the anchor mounting depth h_{ef} and the length of the undercutting head cone formation l were constant. As a result, the distribution of pressure on the rock, in the contact zone of the undercutting head with the rock, was similar in all cases. Hence, the slot trajectories have a similar shape but differ in depth penetration at the initial stage of slot development (depending on the value of the head angle β). As demonstrated in the studies cited above, in this case, the slot initiation point always lies at the corner of the rock undercut for the conical head (point B, Figure 9). Furthermore, as can be seen from Figure 9, there was a rather pronounced dependence of slot propagation on the value of the head cone angle β. Small values of this angle clearly favour deep slot penetration and an increase in the extent of detachment (measured on the free rock surface). In contrast, for breakout anchors, Figure 8 shows that for angle values $\beta \geq 25°$ this relationship is not clear, however, and more detailed research should be carried out to confirm this trend. The changing length of the contact zone of the anchor head with the rock $\boldsymbol{l}$ as well as its orientation relative to the edge of the model appears to be relevant here (β angle). In reality, this will result in the appearance of different values of contact stresses between the rock and the anchor bolt, in each case considered. This also leads to a change in the direction of the resultant force in the rock undercut [41] and can also have an effect on the appearance of microcracks in the medium in this zone, as observed in practice (pseudo-plasticity of the rock medium, sometimes referred to as the rock crushing/concentration

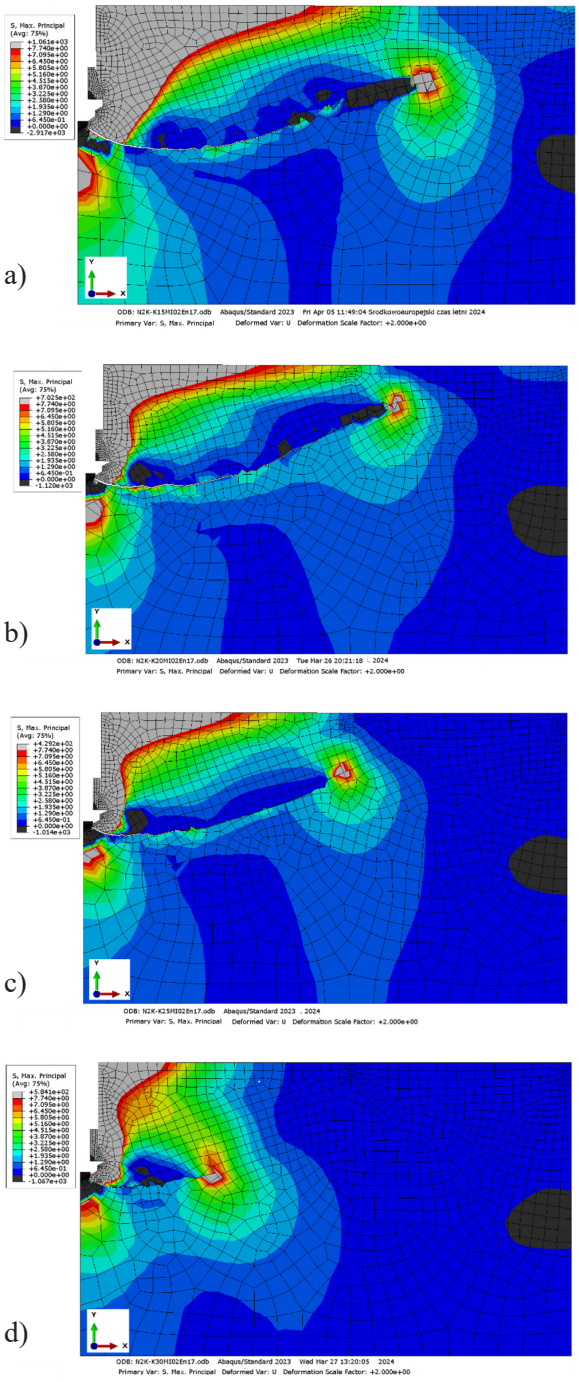

Figure 6. Slot propagation and distribution of maximum main stresses σ_{max}, for the head angle β: (a) $\beta = 15^0$, (b) $\beta = 20^0$, (c) $\beta = 25^0$, (c) $\beta = 30^0$ (scale of deformation =2x)

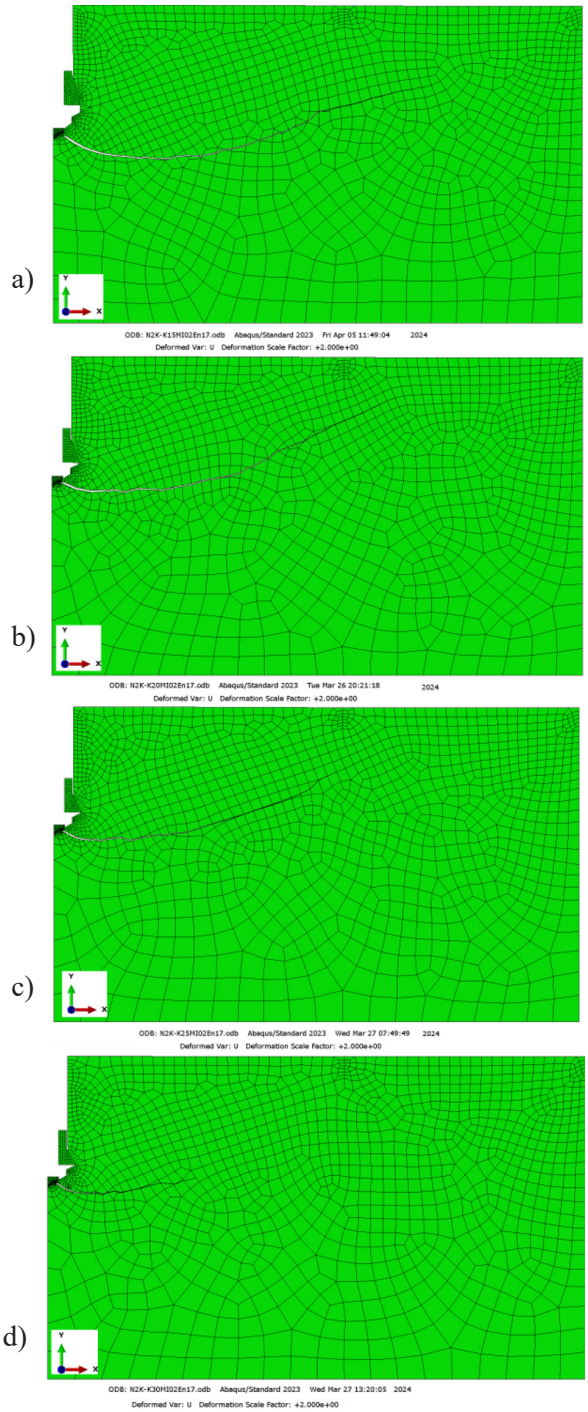

Figure 7. Slot propagation for head angle β: (a) $\beta = 15°$, (b) $\beta = 20°$, (c) $\beta = 25°$, (c) $\beta = 30°$ (scale of deformation = 2x)

zone). As a result, this may translate into observed slot trajectories. As it seems, to some extent, the study [66], confirms the above suggestions. The publication shows [42] that when anchors interact with the medium, the crack propagation mechanism is a function of both the geometrical and boundary conditions of the medium model and the predominant type of cracking can be Type I (tension) cracking or a combination of Type I and Type II (tension and shear) cracking, but never pure Mode II.

The direction of crack propagation is determined from the criterion of the maximum circumferential stress (Fig. 10) given by Equation 11, and the crack propagates when Equation 1 is satisfied [42]:

$$K_I^* sin\theta + K_{II}^*(3cos\theta - 1) = 0 \quad (1)$$

$$cos(\theta/2)\left[K_I^* cos^2(\theta/2) - \frac{3}{2}K_{II}^* sin\theta\right] \geq 1 \quad (2)$$

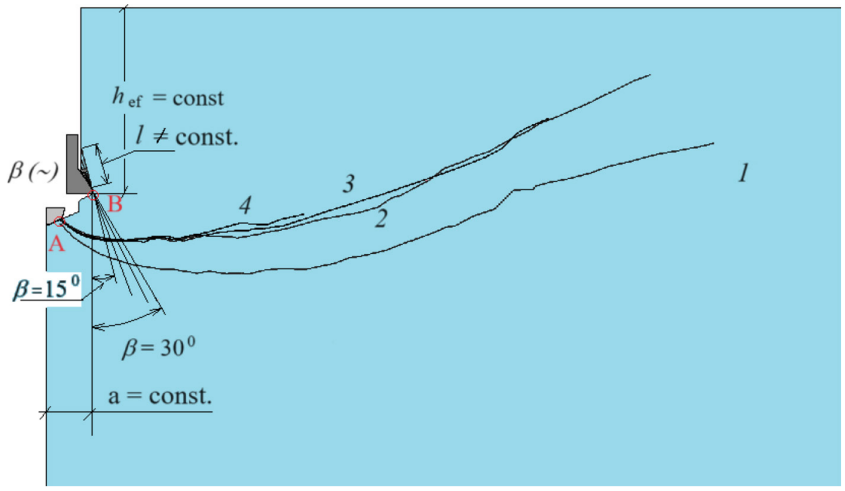

Figure 8. Slot course during damage of the medium structure with the breakout anchor head depending on the value of the head cone angle *β,* where: 1) β = 15°, 2) β = 20°, 3) β = 25°, 3) β = 30°, *a* – radius of the conical head at the base of the cone (= const.), h_{ef} – effective anchor mounting depth (=const.), ν = 0.247, E =14.276 MPa, E_{Ic} = 0.17 N/mm

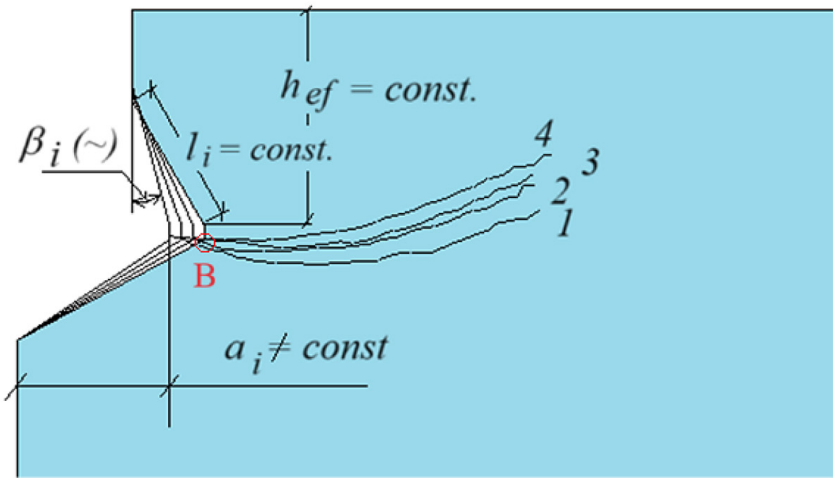

Figure 9. Influence of head angle value β on slot propagation, for: (1) β =15°, (2) β =20°, (3) β = 25°, (4) β = 30°

where:

$$K_I^* = \frac{K_I}{K_{Ic}} \tag{3}$$

$$K_{II}^* = \frac{K_{II}}{K_{Ic}} \tag{4}$$

where: θ – the angle corresponding to the higher maximum circumferential stress is defined as shown in Fig. 10.

As stated in [42], in the processes considered, the tensile damage mode corresponding to K_I* values close to unity generally dominates during crack propagation. During crack growth, however, there are stages where relatively high values of K^*_{II}, are

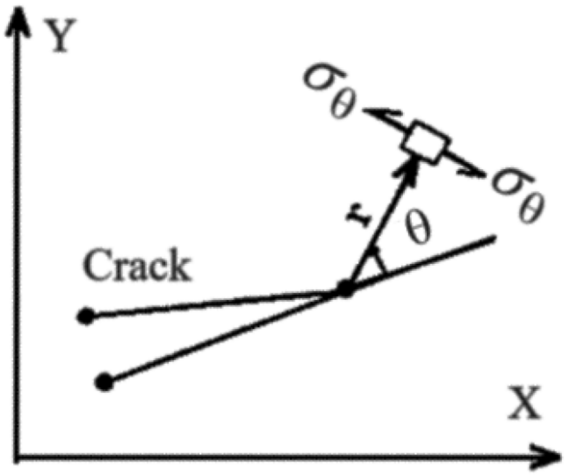

Figure 10. Direction of crack development

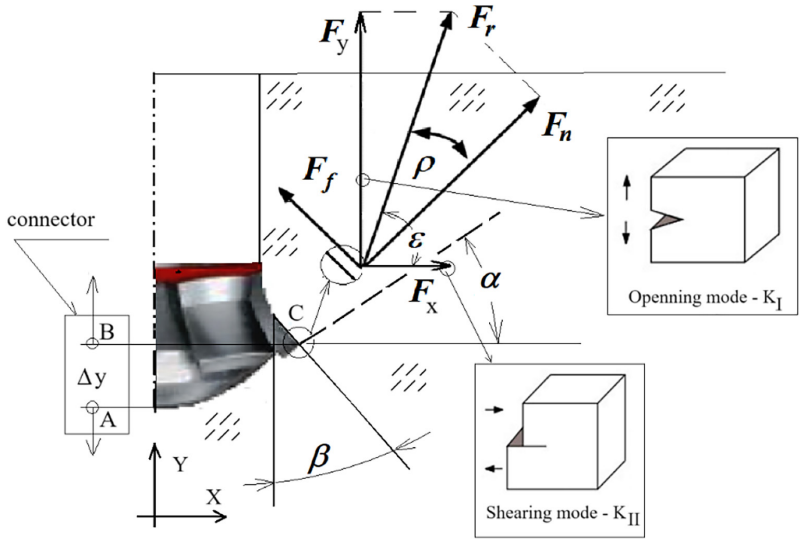

Figure 11. Influence of the components of the breakout anchor head force on the potential occurrence of mixed cracking mode. Components F_x and F_y for the interaction of the anchor conical head and the rock: β – head angle, ρ – friction angle of the head and the rock, F_f – force of friction of the head against the rock (tangential component), F_n – normal component to conical undercutting of the rock, F_r – resultant force of the conical head action on the rock, F_x and F_y – components of the force of the anchor acting on the rock in the accepted coordinate system XY, where Y is in accordance with the anchor axis, ε - the angle of action of the resultant F_r in the adopted coordinate system

obtained, suggesting a change in the cracking mechanism in the damage by tearing out process. In addition to these factors, the grain size of the sandstone may also be important here, as a number of studies have shown that grain size has a significant influence on the development of crack resistance. The issue of slot propagation under the action of a breakout anchor considered here is somewhat similar to the behaviour of the rock overhang subjected to simultaneous bending and shear as described in [67, 68]. There are varying load conditions on the detached rock fragment as the slot develops, which simultaneously translates into changes in the crack resistance of the medium as the crack develops.

With this in mind, further research is planned to analyze the problem in detail, taking into account the possibility of a mixed cracking mode (Mode I + Mode II) during the interaction of the anchor head with the rock, as illustrated in Figure 11.

CONCLUSIONS

Research has confirmed that the possibility of a slot initiation point under the driving bolt end of the breakout anchor, as observed in preliminary tests [34, 57]. athe effect of the value of the angle of the head cone on the trajectory and the extent of the slot formed during the damage of the medium with the head of the breakout anchor. The smaller the value of the head angle β, the greater the range of the breakout. The change of impact of load transmission metod from the head to the rock from the fractured to breakout-undercutting head for breaking occuring in new heads (expanded in the vicinity of the hole bottom – breaking of material) is not unique as regards the point of initiating slots. The impact of the geometrical parameters of the rock undercut model in the vicinity of the bottom of the borehole and the potential clearances between the anchor and the medium there should be further clarified.

REFERENCES

1. Bokor B., Tóth M., Sharma A. Fasteners in Steel Fiber Reinforced Concrete Subjected to Increased Loading Rates. Fibers. 2018; 6(4): 93.
2. Eligehausen R., Mallée R., Silva J.F. Anchorage in concrete construction. Berlin: Ernst; 2006; 378.
3. Tóth M., Bokor B., Sharma A. Anchorage in steel fiber reinforced concrete – concept, experimental evidence and design recommendations for concrete cone and concrete edge breakout failure modes. Engineering Structures. 2019; 181: 60–75.
4. Jonak J., Karpiński R., Wójcik A. Numerical analysis of undercut anchor effect on rock. J Phys: Conf Ser. 2021; 2130(1): 012011.

5. Jonak J., Karpiński R., Wójcik A. Numerical analysis of the effect of embedment depth on the geometry of the cone failure. J Phys: Conf Ser. 2021; 2130(1): 012012.
6. Jonak J., Karpiński R., Wójcik A., Siegmund M. The Influence of the Physical-Mechanical Parameters of Rock on the Extent of the Initial Failure Zone under the Action of an Undercut Anchor. Materials. 2021; 14(8): 1841.
7. Jonak J., Karpiński R., Wójcik A. Influence of the Undercut Anchor Head Angle on the Propagation of the Failure Zone of the Rock Medium. Materials. 2021; 14(9): 2371.
8. Jonak J., Siegmund M., Karpiński R., Wójcik A. Three-Dimensional Finite Element Analysis of the Undercut Anchor Group Effect in Rock Cone Failure. Materials. 2020; 13(6): 1332.
9. Wysmulski P. The effect of load eccentricity on the compressed CFRP Z-shaped columns in the weak post-critical state. Composite Structures. 2022; 301: 116184.
10. Falkowicz K. Numerical Investigations of Perforated CFRP Z-Cross-Section Profiles, under Axial Compression. Materials. 2022; 15(19): 6874.
11. Rogala M., Gajewski J., Gawdzińska K. Crashworthiness analysis of thin-walled aluminum columns filled with aluminum–silicon carbide composite foam. Composite Structures. 2022; 299: 116102.
12. Szabelski J., Karpiński R., Machrowska A. Application of an Artificial Neural Network in the Modelling of Heat Curing Effects on the Strength of Adhesive Joints at Elevated Temperature with Imprecise Adhesive Mix Ratios. Materials. 2022; 15(3): 721.
13. Rogala M. Neural Networks in Crashworthiness Analysis of Thin-Walled Profile with Foam Filling. Adv Sci Technol Res J. 2020; 14(3): 93–9.
14. Gajewski J., Golewski P., Sadowski T. The Use of Neural Networks in the Analysis of Dual Adhesive Single Lap Joints Subjected to Uniaxial Tensile Test. Materials. 2021; 14(2): 419.
15. Jonak J., Karpiński R., Wójcik A., Siegmund M. Numerical Investigation of the Formation of a Failure Cone during the Pullout of an Undercutting Anchor. Materials. 2023; 16(5): 2010.
16. Falkowicz K. Stability and Failure of Thin-Walled Composite Plate Elements with Asymmetric Configurations. Materials. 2024; 17(9): 1943.
17. Rogala M., Tuchowski W., Czarnecka-Komorowska D., Gawdzińska K. Analysis and Assessment of Aluminum and Aluminum-Ceramic Foams Structure. Adv Sci Technol Res J. 2022; 16(4): 287–97.
18. Krauze K., Mucha K., Wydro T., Pieczora E. Functional and Operational Requirements to Be Fulfilled by Conical Picks Regarding Their Wear Rate and Investment Costs. Energies. 2021; 14(12): 3696.
19. Biały W. Assessment of the technical state of mining machinery and devices with the use of diagnostic methods. Production Engineering Archives. 2024; 30(2): 266–72.
20. Kotwica K., Stopka G., Wieczorek A.N., Kalita M., Bałaga D., Siegmund M. Development of Longwall Shearers' Haulage Systems as an Alternative to the Eicotrack System Used Nowadays. Energies. 2023; 16(3): 1402.
21. Waloski R., Korzeniowski W., Bołoz Ł., Rączka W. Identification of Rock Mass Critical Discontinuities While Borehole Drilling. Energies. 2021; 14(10): 2748.
22. HILTI. Technisches Handbuch der Befestigungstechnik für Hoch- und Ingenieurbau. Ausgabe; HILTI: Schaan, Liechtenstein, 2016.
23. Siegmund M., Kalita M., Bałaga D., Kaczmarczyk K., Jonak J. Testing the rocks loosening process by undercutting anchors. Studia Geotechnica et Mechanica. 2020; 42(3): 276–90.
24. Al-Ta A.S., Mohammed A. Tensile Strength of Short Headed Anchors Embedded in Steel Fibrous Concrete. (AREJ). 2010; 18(5): 35–49.
25. Albadran S.Q. Performance of Cast-in Anchors in Early Age Concrete. Swinburne University of Technology; 2020.
26. Bokor B., Sharma A., Hofmann J. Experimental investigations on concrete cone failure of rectangular and non-rectangular anchor groups. Engineering Structures. 2019; 188: 202–17.
27. Cajka R., Marcalikova Z., Bilek V., Sucharda O. Numerical Modeling and Analysis of Concrete Slabs in Interaction with Subsoil. Sustainability. 2020; 12(23): 9868.
28. Cusatis G., Di Luzio G., Rota M. Simulation of headed anchor failure. In: Computational Modeling of Concrete Structures (Proc, EURO-C 2003 Conference), St Johann im Pongau, Austria. 2003; 683–8.
29. Benedetti L., Cervera M., Chiumenti M. High-fidelity prediction of crack formation in 2D and 3D pullout tests. Computers & Structures. 2016; 172: 93–109.
30. Brincker R., Ulfkjær J.P., Adamsen P., Langvad L., Toft R. Analytical model for hook anchor pull-out. In: Proceedings of the International Symposium on Anchors in Theory and Practice: Salzburg, Austria, 9-10 october 1995. CRC Press/Balkema; 1995; 3–15.
31. Gontarz J., Podgórski J., Siegmund M. Comparison of crack propagation analyses in a pull-out test. In Lublin, Poland; 2018 [cited 2022 Jan 20]. p. 130011. Available from: http://aip.scitation.org/doi/abs/10.1063/1.5019141
32. Hariyadi, Munemoto S., Sonoda Y. Experimental Analysis of Anchor Bolt in Concrete under the Pull-Out Loading. Procedia Engineering. 2017; 171: 926–33.
33. Chen Z. Analyzing the failure mechanisms and developing strength prediction models for concrete

expansion and screw anchors in tension. Washington State University; 2018.

34. Jonak J., Karpiński R., Siegmund M., Wójcik A., Jonak K. Analysis of the Rock Failure Cone Size Relative to the Group Effect from a Triangular Anchorage System. Materials. 2020; 13(20): 4657.
35. Al-Yousuf A., Pokharel T., Lee J., Gad E., Abdouka K., Sanjayan J. Performance of cast-in anchors in early age concrete with supplementary cementitious materials. Mater Struct. 2023; 56(1): 2.
36. Karmokar T., Mohyeddin A., Lee J., Paraskeva T. Concrete cone failure of single cast-in anchors under tensile loading – A literature review. Engineering Structures. 2021; 243: 112615.
37. Di Nunzio G., Muciaccia G. Cast-in-place fasteners under tensile loading: A critical review. Structures. 2022; 41: 1532–45.
38. Bao Q.T., Lee K., An H., Lee D.H., Shin J. Effective prediction finite element model of pull-out capacity for cast-in-place anchor in high strain rate effects. Sci Rep. 2023; 13(1): 18070.
39. Meloni D., De Nicolo B., Valdes M. Finite Element Model of the Pull-Out Test for Concrete Strength Evaluation. In Cagliari, Sardinia, Italy; [cited 2024 May 17]. p. 167. Available from: http://www.ctresources.info/ccp/paper.html?id=7500
40. Jeon S., Ju M., Park J., Choi H., Park K. Prediction of concrete anchor pull-out failure using cohesive zone modeling. Construction and Building Materials. 2023 Jun;383:130993.
41. Jonak J, Karpiński R, Wójcik A, Siegmund M. The Effect of Undercut Anchor Diameter on the Rock Failure Cone Area in Pullout Tests. Adv Sci Technol Res J. 2022; 16(5): 261–70.
42. Chahrour A.H., Ohtsu M. Analysis of anchor bolt pullout tests by a two-domain boundary element method. Materials and Structures. 1995; 28(4): 201–9.
43. Wysmulski P. Analysis of the Effect of an Open Hole on the Buckling of a Compressed Composite Plate. Materials. 2024; 17(5): 1081.
44. Wysmulski P., Mieczkowski G. Influence of Size of Open Hole on Stability of Compressed Plate Made of Carbon Fiber Reinforced Polymer. Adv Sci Technol Res J. 2024; 18(2): 238–47.
45. Falkowicz K., Kuciej M., Świech Ł. Temperature Effect on Buckling Properties of Thin-Walled Composite Profile Subjected to Axial Compression. Adv Sci Technol Res J. 2024; 18(3): 305–13.
46. Chessa J., Smolinski P., Belytschko T. The extended finite element method (XFEM) for solidification problems. Numerical Meth Engineering. 2002; 53(8): 1959–77.
47. Belytschko T., Black T. Elastic crack growth in finite elements with minimal remeshing. International journal for numerical methods in engineering. 1999; 45(5): 601–20.
48. Wysmulski P. Numerical and Experimental Study of Crack Propagation in the Tensile Composite Plate with the Open Hole. Adv Sci Technol Res J [Internet]. 2023;17(4). Available from: http://www.astrj.com/Numerical-and-Experimental-Study-of-Crack-Propagation-in-the-Tensile-Composite-Plate,169970,0,2.html
49. Pathak H., Singh A., Singh I.V. Fatigue crack growth simulations of 3-D problems using XFEM. International Journal of Mechanical Sciences. 2013; 76: 112–31.
50. Lecampion B. An extended finite element method for hydraulic fracture problems. Commun Numer Meth Engng. 2009; 25(2): 121–33.
51. Areias P.M.A., Belytschko T. Non-linear analysis of shells with arbitrary evolving cracks using XFEM. Numerical Meth Engineering. 2005; 62(3): 384–415.
52. Backers T., Stephansson O., Rybacki E. Rock fracture toughness testing in Mode II—punch-through shear test. International Journal of Rock Mechanics and Mining Sciences. 2002; 39(6): 755–69.
53. Bahrami B., Nejati M., Ayatollahi M.R., Driesner T. Theory and experiment on true mode II fracturing of rocks. Engineering Fracture Mechanics. 2020; 240: 107314.
54. Wei M.D., Dai F., Xu N.W., Liu Y., Zhao T. Fracture prediction of rocks under mode I and mode II loading using the generalized maximum tangential strain criterion. Engineering Fracture Mechanics. 2017; 186: 21–38.
55. Emami Meybodi E., Hussain S.K., Fatehi Marji M., Rasouli V. Application of machine learning models for predicting rock fracture toughness mode-I and mode-II. Journal of Mining and Environment. 2022; 13(2): 465–80.
56. Falkowicz K., Kulisz M. Prediction of Buckling Behaviour of Composite Plate Element Using Artificial Neural Networks. Adv Sci Technol Res J. 2024; 18(1): 231–43.
57. Jonak J., Karpiński R., Wójcik A., Siegmund M., Kalita M. Determining the Effect of Rock Strength Parameters on the Breakout Area Utilizing the New Design of the Undercut/Breakout Anchor. Materials. 2022; 15(3): 851.
58. Fuchs W., Eligehausen R., Breen J.E. Concrete capacity design (CCD) approach for fastening to concrete. Structural Journal. 1995; 92(1): 73–94.
59. Jonak J., Karpiński R., Siegmund M., Machrowska A., Prostański D. Experimental Verification of Standard Recommendations for Estimating the Load-carrying Capacity of Undercut Anchors in Rock Material. Advances in Science and Technology Research Journal [Internet]. 2021 Jan 11; Available from: http://www.astrj.com/Experimental-Verification-

of-Standard-Recommendations-for-Estimating-the-Load-carrying,132279,0,2.html

60. Walter H., Baillet L., Brunet M. Contact analysis for the modelling of anchors in concrete structures. WIT Transactions on Engineering Sciences. 1997; 14.
61. Gontarz J., Podgórski J., Jonak J., Kalita M., Siegmund M. Comparison Between Numerical Analysis and Actual Results for a Pull-Out Test. [cited 2021 Mar 30]; Available from: http://et.ippt.pan.pl/index.php/et/article/view/1005
62. Jonak J., Karpiński R., Wójcik A. Influence of Anchor Depth and Friction Coefficient Between Anchor and Rock on the Trajectory of Rock Masses Detachment. Adv Sci Technol Res J. 2023 Aug 16; 17(4): 290–8.
63. Wysmulski P. Non-linear analysis of the postbuckling behaviour of eccentrically compressed composite channel-section columns. Composite Structures. 2023 Feb; 305: 116446.
64. Falkowicz K. Experimental and numerical failure analysis of thin-walled composite plates using progressive failure analysis. Composite Structures. 2023; 305: 116474.
65. Jonak J., Karpiński R., Wójcik A. Influence of the Undercut Anchor Head Angle on the Propagation of the Failure Zone of the Rock Medium—Part II. Materials. 2021;14(14): 3880.
66. Furche J., Eligehausen R. Lateral blow-out failure of headed studs near a free edge. 1991 [cited 2021 Feb 22]; Available from: http://elib.uni-stuttgart.de/handle/11682/449
67. Wu L.Z., Shao G.Q., Huang R.Q., He Q. Overhanging Rock: Theoretical, Physical and Numerical Modeling. Rock Mech Rock Eng. 2018; 51(11): 3585–97.
68. Huang R.Q., Wu L.Z., He Q., Li J.H. Stress Intensity Factor Analysis and the Stability of Overhanging Rock. Rock Mech Rock Eng. 2017; 50(8): 2135–42.